A&A 375, 1049–1061 (2001)
DOI: 10.1051/0004-6361:20010908

Astronomy & Astrophysics

Statistical analysis of solar Hα flares

M. Temmer[1], A. Veronig[1], A. Hanslmeier[1], W. Otruba[2], and M. Messerotti[3]

[1] Institut für Geophysik, Astrophysik & Meteorologie, Universität Graz, Universitätsplatz 5, 8010 Graz, Austria
[2] Sonnenobservatorium Kanzelhöhe, 9521 Treffen, Austria
[3] Osservatorio Astronomico di Trieste, Via G. B. Tiepolo 11, 34131 Trieste, Italy

Received 24 April 2001 / Accepted 12 June 2001

Abstract. A statistical analysis of a large data set of Hα flares comprising almost 100 000 single events that occurred during the period January 1975 to December 1999 is presented. We analyzed the flares evolution steps, i.e. duration, rise times, decay times and event asymmetries. Moreover, these parameters characterizing the temporal behavior of flares, as well as the spatial distribution on the solar disk, i.e. N-S and E-W asymmetries, are analyzed in terms of their dependency on the solar cycle. The main results are: 1) The duration, rise and decay times increase with increasing importance class. The increase is more pronounced for the decay times than for the rise times. The same relation is valid with regard to the brightness classes but in a weaker manner. 2) The event asymmetry indices, which characterize the proportion of the decay to the rise time of an event, are predominantly positive (≈90%). For about 50% of the events the decay time is even more than 4 times as long as the rise time. 3) The event asymmetries increase with the importance class. 4) The flare duration and decay times vary in phase with the solar cycle; the rise times do not. 5) The event asymmetries do not reveal a distinct correlation with the solar cycle. However, they drop during times of solar minima, which can be explained by the shorter decay times found during minimum activity. 6) There exists a significant N-S asymmetry over longer periods, and the dominance of one hemisphere over the other can persist for more than one cycle. 7) For certain cycles there may be evidence that the N-S asymmetry evolves with the solar cycle, but in general this is not the case. 8) There exists a slight but significant E-W asymmetry with a prolonged eastern excess.

Key words. methods: statistical – Sun: activity – Sun: flares

1. Introduction

With the discovery of the first solar flare observed independently by R. C. Carrington and R. Hodgson on September 1, 1859, knowledge about these energetic phenomena on the Sun has steadily increased. The statistical investigations of the characteristics of solar Hα flares essentially started in the 1930s, when a worldwide surveillance of the Sun based on Hale's spectrohelioscope was established (Cliver 1995). Since then many papers have been published analyzing different statistical aspects of solar flares. However, in most of the papers only single aspects are investigated and/or the data set comprises a quite limited period. Moreover, there exists no recent paper extensively studying the statistical properties of solar Hα flares.

In the present paper we make use of the substantial data collection of solar Hα flares in the Solar Geophysical Data (SGD). We selected the period January 1975 (since then the Hα flares are listed with the same content and format) to December 1999. With this selection we have a homogeneous data set comprising almost 100 000 single flare events, which provides a significant statistical basis. Furthermore, as the selected period entirely covers two solar cycles, 21 and 22, and the rising phase of solar cycle 23 until the end of year 1999, the data set also enables us to analyze dependency of the flare characteristics on the solar cycle.

The paper is structured as follows. In Sect. 2 a characterization of the data set is given. Section 3 describes the applied methods. In Sect. 4 the results are presented and discussed, comprising a statistical analysis of the temporal flare parameters combining the data of the overall period, such as flare duration, rise times, decay times (Sect. 4.1) and event asymmetries (Sect. 4.2). Also, we analyze the above-mentioned temporal and spatial flare characteristics, namely the N-S and E-W asymmetry, and its dependency on the solar cycle (Sect. 4.3). Section 5 contains a summary of the main results and the conclusions.

2. Data

For the present analysis we make use of the Hα flares listed in the SGD for January 1975 to December 1999. During this period the occurrence of 97 894 Hα flare events is reported. Table 1 lists the number of flares with respect to

Send offprint requests to: A. Veronig,
e-mail: asv@igam06ws.KFUniGraz.ac.at

Table 1. The number of flare events for the different importance classes (S, 1, 2, 3, 4) and the corresponding percentage values are listed. T denotes the total number of flares occurring in the period 1975 to 1999, for which the importance class is reported.

Importance	No. of events	No. (%)
S	85 649	89.27
1	9176	9.56
2	1014	1.05
3	101	0.11
4	5	0.01
T	95 945	100.00

Table 2. The number of flare events for the different brightness classes (f, n, b) and the corresponding percentage values are listed. T denotes the total number of flares occurring in the period 1975 to 1999, for which the brightness class is reported.

Brightness	No. of events	No. (%)
f	59 973	61.42
n	31 454	32.22
b	6208	6.36
T	97 635	100.00

the different importance classes, denoting the flare size, i.e. subflares (S), flares of importance 1, 2, 3 and 4. In Table 2 the number of flares is subdivided into the three brightness classes, characterizing the intensity of the flare emission in Hα, i.e. f(aint), n(ormal) and b(right) flares. Note that the total number of flare events subdivided into importance classes and brightness classes differs from each other as well as from the overall number of reported flares due to incomplete early flare reports, where for some events the importance class and/or the brightness class is not given.

It can be clearly seen in Table 1 that the percentage of flares of importance 2, 3, and 4 is very small, covering only ≈1.2% of the overall number of events. Especially during periods of minimum solar activity, their number is vanishing. Therefore, to ensure a statistically meaningful data set, for the analysis these three importance classes are merged into one group, denoted as >1.

In Table 3 we list the number of flares belonging to the different groups of importance and brightness classes, resulting in nine subclasses. The table clearly reveals that the importance and brightness classes show a strong interdependence. Subflares have a strong tendency to be faint, importance 1 flares to be of normal brightness and importance >1 flares to be of bright or normal brightness. Therefore, in the detailed analysis we do not consider the partitioning of flares with respect to all the subclasses but only with respect to the importance classes. The choice of the importance instead of the brightness classes is motivated by the fact that the importance classes are determined in a more objective way, i.e. the measured area of a flare, than the brightness classes, i.e. the subjective estimation of the flare intensity by the observer.

The present statistical analysis deals with temporal as well as spatial characteristics of Hα flares. For the

Table 3. The number of flare events for the different brightness (f, n, b) and importance (S, 1, > 1) classes, given in absolute values and percentages of the respective importance class.

	S		Imp. 1		Imp. >1	
f	56 806	(66.39%)	2251	(24.69%)	85	(7.65%)
n	25 050	(29.28%)	5098	(55.93%)	478	(43.02%)
b	3706	(4.33%)	1767	(19.38%)	548	(49.33%)
T	85 562	(100.00%)	9116	(100.00%)	1111	(100.00%)

analysis of temporal flare parameters, such as duration, rise times, decay times and event asymmetries, we make use of letter codes listed in the SGD, which describe the quality of the reported start, end and maximum times. The qualifiers "U", "E" and "D" indicate that the given time is uncertain, the event started before or ended after the reported time. Additionally, digit qualifiers are annotated (from 1 to 9, given in minutes), which describe the spread among the times reported by different observatories. An asterisk denotes a spread of more than 9 min.

For the analysis of temporal flare parameters events marked with an "U", "E", "D" or an asterisk are discarded, in order to prevent biases due to uncertainties in the reported times. Since the data set is quite huge, this rejection of data has no distinct influence on the statistics. Applying these selection criteria, we get 75 739 Hα flare events with reported importance class, covering 68 948 subflares (91.0%), 6169 flares of importance 1 (8.2%) and 622 of importance >1 (0.8%). For the flares with reported brightness class 76 975 events are obtained. Note that for the analysis of spatial flare parameters, such as N-S and E-W asymmetries, the original data set as listed in Tables 1 and 2 is used.

3. Analysis and methods

3.1. Calculated parameters

The Hα flares that occurred within the considered time span are statistically analyzed with respect to their temporal evolution. From the evolution steps that are observed within a flare event, i.e., start time $t_{\rm start}$, end time $t_{\rm end}$ and maximum time $t_{\rm max}$, we calculated the duration ($t_{\rm end} - t_{\rm start}$), the rise time ($t_{\rm max} - t_{\rm start}$) and the decay time ($t_{\rm end} - t_{\rm max}$). Furthermore, in order to characterize the proportion of the rise and the decay time of a flare event, we computed the event asymmetry index $A_{\rm ev}$ (Pearce et al. 2001), defined as

$$A_{\rm ev} = \frac{t_{\rm decay} - t_{\rm rise}}{t_{\rm decay} + t_{\rm rise}}, \quad (1)$$

with $t_{\rm rise}$ the rise time and $t_{\rm decay}$ the decay time. The event asymmetry index is a dimension-less quantity within the range $[-1, +1]$. A value close to zero states that the rise and the decay time are roughly equal. The larger the deviation from zero, the more asymmetric is the evolution of a flare, whereas positive values indicate that the decay phase is longer than the rising phase, for negative values, the opposite.

Furthermore, we analyzed the occurrence frequency of solar flares in relation to the solar hemispheres. It is customary among authors who are investigating N-S and E-W asymmetries to compute the respective asymmetry indices (Letfus 1960). The N-S asymmetry index $A_{\rm NS}$ is defined as

$$A_{\rm NS} = \frac{n_{\rm N} - n_{\rm S}}{n_{\rm N} + n_{\rm S}}\,, \tag{2}$$

with $n_{\rm N}$ and $n_{\rm S}$ the number of flares occurring in the northern and southern hemisphere, respectively. The E-W asymmetry index $A_{\rm EW}$ is defined analogously. Asymmetry indices close to zero indicate an equal distribution of flares with respect to the hemispheres. Positive values of the N-S and the E-W asymmetry index characterize an excess of flares in the northern and the eastern hemisphere, respectively.

3.2. Statistical measures

According to the distributions of the various temporal flare parameters, which are calculated in the frame of this analysis, the determination of the average values was chosen differently from the commonly used arithmetic mean. Since the relevant distributions are significantly asymmetric (see Figs. 1–3), the average is better represented by the median instead of the arithmetic mean. Moreover, the median is more insensitive with respect to extreme data values than the arithmetic mean. The median $\tilde{x}$ of a distribution of values $\{x_i\}$ is given by that value, which has equal numbers of values above and below it. Note that for distributions with positive skewness the median value is smaller than the arithmetic mean, whereas for distributions with negative skewness it is larger.

Furthermore, as a robust measure of dispersion we applied the median absolute deviation, which is more appropriate for the kind of distributions we are dealing with than the standard deviation. The median absolute deviation $\tilde{D}$ is defined as

$$\tilde{D} = \text{Median}\{|x_i - \tilde{x}|\}\,, \tag{3}$$

where $\{x_i\}$ denote the data values and $\tilde{x}$ is the median of the $\{x_i\}$. Additionally, we also make use of the 95% confidence interval, which gives the probability that for a frequent use of the applied procedure (which is legitimated by the huge data set), 95% of the data are gathered within the confidence limits. A conservative 95% confidence interval for the median is given by a rule of thumb as $\tilde{x} \pm c_{95}$ with

$$c_{95} = \frac{1.58\ (Q_3 - Q_1)}{\sqrt{n}}. \tag{4}$$

Q_1 and Q_3 denote the first and the third quartile, respectively, n the total number of data values. The first quartile Q_1, or 25th percentile, of a distribution is given by that value which has 25% of values below it; the third quartile Q_3, or 75th percentile, is given by the value with 75% of values below it. Note that the median $\tilde{x}$ is identical to the second quartile Q_2, or 50th percentile.

Table 4. Mean, median, mode and 90th percentile values of the duration, rise and decay times of the total number of flares considered.

Stat. measure	Duration (min)	Rise time (min)	Decay time (min)
Mean	20.6	5.1	15.5
Median	15.0	3.0	11.0
Mode	8.0	1.0	8.0
P_{90}	55.0	11.0	31.0

To specify the statistical significance of the N-S and E-W asymmetry indices, we followed Letfus (1960). The dispersion of the N-S asymmetry of a random distribution of flares is given by

$$\Delta A_{\rm NS} = \pm \frac{1}{\sqrt{2(n_{\rm N} + n_{\rm S})}}\,, \tag{5}$$

which depends on the total number of flares occurring in the northern and the southern hemisphere, respectively. To verify the reliability of the observed N-S asymmetry values, a χ^2 test is applied with

$$\chi = \frac{2(n_{\rm N} - n_{\rm S})}{\sqrt{(n_{\rm N} + n_{\rm S})}} = \frac{\sqrt{2} A_{\rm NS}}{\Delta A_{\rm NS}}. \tag{6}$$

If $A_{\rm NS} = 2\Delta A_{\rm NS}$, the probability that the observed N-S asymmetry exceeds the dispersion value of a random distribution is $p = 99.5\%$, specifying asymmetry values which are highly significant. The same test, calculating the corresponding quantities, is also applied to the E-W asymmetry indices.

4. Results and discussion

4.1. Duration, rise and decay time

Figure 1 shows the distributions of the duration, rise and decay times calculated from all flares reported for the period 1975–1999, which fulfilled the quality criteria regarding start, end and maximum time stated in Sect. 2. All distributions reveal a pronounced positive skewness. The overplotted solid line indicates the median value of the respective distribution. The dashed line indicates the 90th percentile P_{90}, which states that only 10% of the events have a value larger than P_{90}. In Table 4 we give a list of various statistical measures characterizing the duration, rise and decay times of the data set, namely the arithmetic mean, the median, the mode (i.e. the most frequently occurring value), and the 90th percentile P_{90}.

Figure 2 shows the distributions of the flare duration separately for the different groups of importance classes, i.e., S, 1 and >1. Table 5 summarizes the median values of the duration, rise and decay times with respect to the different importance classes. Additionally, the 95% confidence interval and the absolute median deviation are given. For the sake of completeness, in Table 6 the same

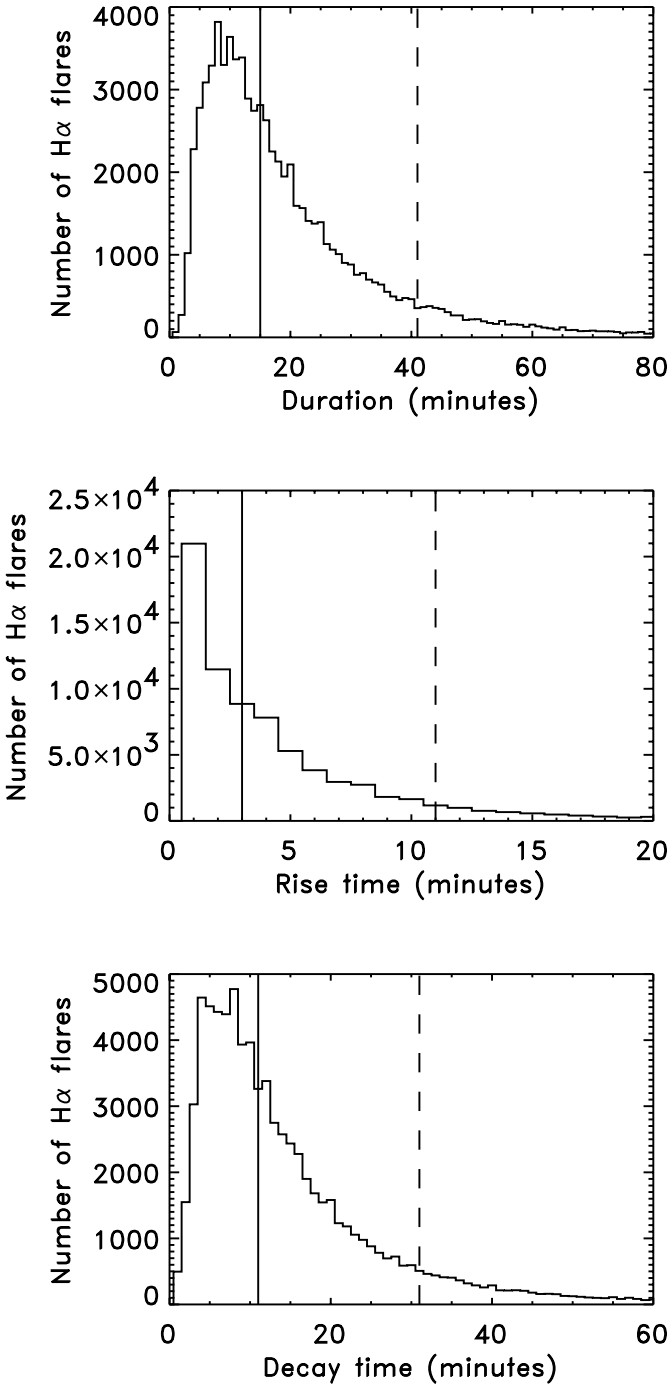

Fig. 1. Histograms of duration, rise and decay times calculated from the overall number of flares during 1975–1999 fulfilling the given quality criteria. The solid line indicates the median value of the distribution, the dashed line the 90th percentile. (Note, that for the sake of clearness, the ranges of the abscissa axes are cut off.)

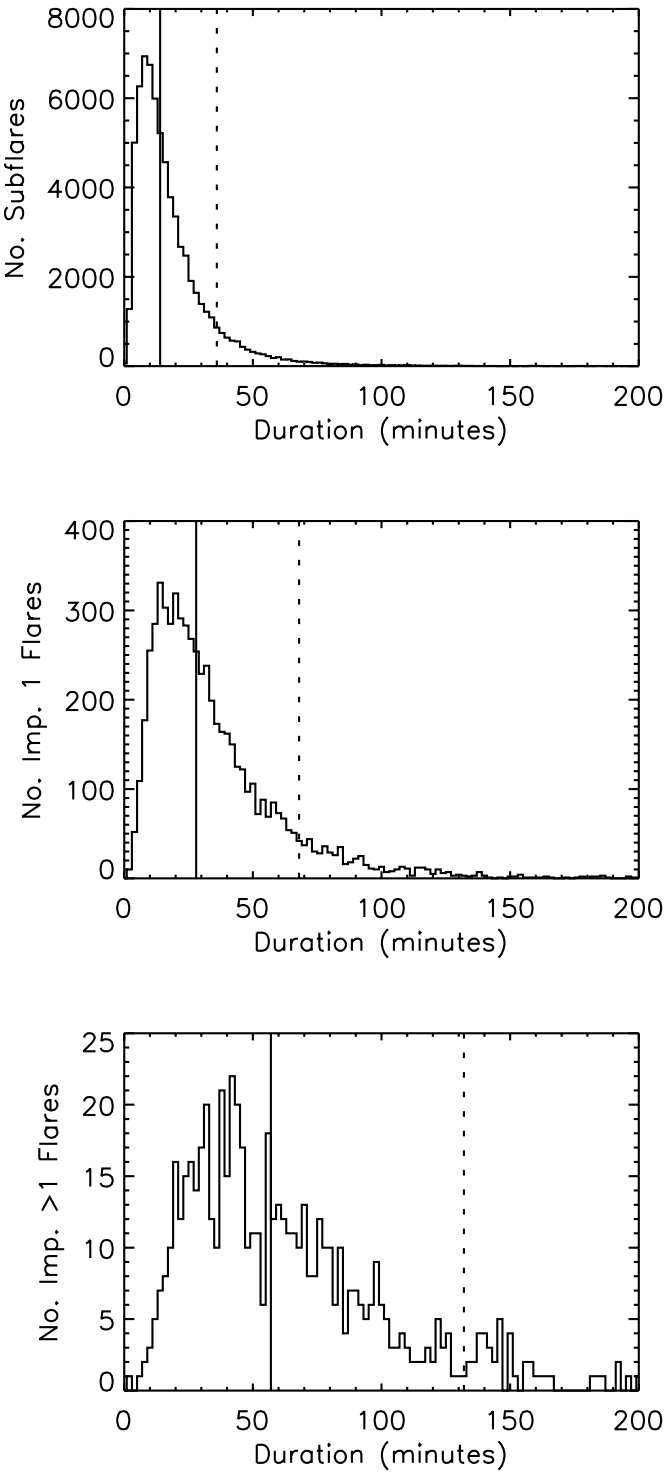

Fig. 2. Histograms of flare duration for the different importance classes (S, 1, > 1). The solid line indicates the median value of the distribution, the dashed line the 90th percentile.

quantities are listed with regard to the different brightness classes. As Table 5 clearly reveals, the duration, rise and decay times increase with the importance class. The same, even if less pronounced, holds for the brightness classes, providing further evidence that the importance and brightness classes are interdependent classification schemes.

The finding that the flare duration increases with increasing importance class, hence with the flare area, is reported by a number of papers (cf. Table 7). Contrary to that, by means of a scatter plot analysis of flare duration versus flare area of an overall number of 16 324 events, Yeung & Pearce (1990) pointed out that there is a

Table 5. Median values with 95% confidence interval, $\tilde{x} \pm c_{95}$, and absolute median deviation $\tilde{D}$ of the duration, rise and decay times for the different importance classes (S, 1, >1) and the total number of flares (T). All values are given in minutes. (Note that due to the nonlinearity of the median the sum of the rise and decay time does not exactly render the duration.)

Imp.	Duration		Rise time		Decay time	
	$\tilde{x} \pm c_{95}$	$\tilde{D}$	$\tilde{x} \pm c_{95}$	$\tilde{D}$	$\tilde{x} \pm c_{95}$	$\tilde{D}$
S	14.0 ± 0.1	6.0	3.0 ± 0.1	2.0	10.0 ± 0.1	5.0
1	28.0 ± 0.5	12.0	5.0 ± 0.1	3.0	22.0 ± 0.5	10.0
>1	57.0 ± 3.2	24.0	8.0 ± 0.6	4.0	45.0 ± 2.9	21.0
T	15.0 ± 0.1	7.0	3.0 ± 0.1	2.0	11.0 ± 0.1	5.0

Table 6. Median values with 95% confidence interval, $\tilde{x} \pm c_{95}$, and absolute median deviation $\tilde{D}$ of the duration, rise and decay times for the different brightness classes (f, n, b) and the total number of flares (T). All values are given in minutes.

Bright.	Duration		Rise time		Decay time	
	$\tilde{x} \pm c_{95}$	$\tilde{D}$	$\tilde{x} \pm c_{95}$	$\tilde{D}$	$\tilde{x} \pm c_{95}$	$\tilde{D}$
f	13.0 ± 0.1	6.0	3.0 ± 0.1	2.0	10.0 ± 0.5	5.0
n	19.0 ± 0.2	9.0	4.0 ± 0.2	2.0	14.0 ± 0.2	7.0
b	24.0 ± 0.6	12.0	4.0 ± 0.1	2.0	19.0 ± 0.5	10.0
T	15.0 ± 0.1	7.0	3.0 ± 0.1	2.0	11.0 ± 0.1	5.0

continuous distribution of flare duration and flare area, concluding that there is no evidence for more than one class of Hα flares and that there is no correlation between flare area and duration. However, as can be seen in Fig. 2, the distributions of the flare duration reveal distinct differences for the different classes. For subflares, the distribution reveals a larger skewness and the maximum of the distribution is located at smaller values than for larger flares. We suspect that the continuous distribution of flare duration and flare area found by Yeung & Pearce (1990) results from the fact that most of the flares are subflares (≈90%). Although the relative number of subflares of long duration is very small (see Fig. 2, top panel), their absolute number is still higher than those of large flares. (Due to the different scales of the ordinate this fact does not show up in Fig. 2.) Thus, if all flares are considered together, it is not possible to separate the different distributions of different flare classes and the analysis is mainly determined by the behavior of the subflares, which intrinsically prevents detection of more than one class of flare events.

In Table 7 we give an overview of the studies of flare duration that were carried out previously. Since in most papers the arithmetic mean is used, we list in Table 7 the mean values of the duration. For the present analysis, we obtained the following mean values for the flare duration: 18.9 min for subflares, 35.7 min for importance 1, 66.3 min for importance 2 and 116.0 min for importance 3 flares. For importance 4 flares we do not specify a mean value as out of the four events of this class reported during the considered period, only one event fulfilled the quality criteria given in Sect. 2.

As can be seen in Table 7, the duration values obtained by the different authors reveal a quite large dispersion. The reasons for this can be manifold. One possible reason is given by observational selection effects which are changing over the years. E.g., increasing time cadences in the solar flare patrol lead to an increase in the number of detected short-lived events, most of them subflares. Another aspect might be the fact that in the miscellaneous studies, different data sets are used, in which start, maximum and end times of a flare have been derived/defined by different criteria. Moreover, it has to be considered that the flare classification scheme has changed, from (1, 2, 3) over (1−, 1, 2, 3, 3+) to (S, 1, 2, 3, 4), which sometimes leads to a mismatch in the comparison of values. (E.g., the old importance 1 class may comprise importance 1 flares as well as subflares.) Finally, there may be also physical reasons, i.e., the average flare characteristics, such as flare duration, may change in the course of the solar cycle.

As we have a homogeneous data set at our disposal (for the data collected in the SGD a constant classification scheme and a well-defined methodology to derive start, end and maximum times is in use), covering more than two solar cycles, we were able to analyze the temporal flare parameters as a function of the solar cycle (Sects. 4.3.2 and 4.3.3), with the objective to determine if there are indeed physical changes in the temporal flare characteristics.

4.2. Event asymmetry

Hα flares do not reveal a symmetrical behavior regarding their temporal evolution, i.e. the rise time is not the same as the decay time. With the use of the event asymmetry index defined by Eq. (1) we investigate this behavior quantitatively. Figure 3 shows the distributions of the event asymmetries calculated for the different importance classes. All distributions reveal a pronounced negative skewness, i.e. an accumulation at positive values, showing that for the majority of events the decay phase is significantly longer than the rising phase.

In Table 8 we list the median values of the event asymmetries for the different importance classes, as well as the 95% confidence intervals, the absolute median deviations, and the 10th percentiles. It can be seen that the asymmetries increase with increasing importance class. Since the differences of event asymmetries between the various classes are larger than the 95% confidence intervals, the effect can be considered as statistically significant. For the total number of events we obtain a median event asymmetry of ≈0.6, which implies that for about 50% of the events the decay phase is more than 4 times as long as the rising phase. A value of $P_{10} \approx 0.0$ means that only about 10% of all flares have a shorter decay than rise time. Considering only flares of importance >1, we obtain for $P_{10} \approx 0.2$, stating that for about 90% of that type of events, the decay time is even more than 1.5 times the rise time.

Table 7. Mean values of flare duration calculated by different authors (given in minutes), listed for the total number of flares (T) as well as separately for the importance classes (S, 1, 2, 3, 4) if available. We list also the period of data record and the total number of flares, on which the studies are based. Note that in particular for papers published before 1966, i.e. the year in which the current flare notation was constituted, importance class 1 may also comprise subflares (in former notation: 1−) and class 3 may also comprise class 4 events (in former notation: 3+). In cases, in which it was possible to recover this fact, the concerned importance class is transformed to the present notation.

Author(s)	Period	No. of flares	Mean duration					
			S	1	2	3	4	T
Newton & Barton[1] (1937)	1935–1936	—	—	—	—	—	—	20.0–40.0
Waldmeier (1938)	1935–1937	357	—	21.0	38.0	61.0	—	27.0
Giovanelli (1948)	1937–1938	24	—	—	—	—	—	30.0
Waldmeier (1948)	1935–1944	927	—	20.3	33.4	62.4	—	24.8
Ellison (1949)	1935–1947	109	—	17.0	29.0	62.0	∼180.0	—
Warwick (1954)	1951–1953	357	31.0		60.0 (≥1)			40.0
Dodson et al.[2] (1956)	1949–1952	194	28.0	43.0	66.0	84.0		—
Waldmeier & Bachmann (1959)	1945–1954	1604	—	22.1	44.8	84.9	—	—
Smith (1962)	1935–1954	—	—	20.3	33.4	62.4	—	—
Reid (1968)	1958–1965	2907	16.5	28.2		60.5 (≥2)		—
Ružičková-Topolová[3] (1974)	1957–1965	661	—	—	71.3	129.9	305.5	—
Wilson (1983)	1980	1348	—	—	—	—	—	29.8
Antalová (1985)	1970–1974	460	27.0	55.0	78.0	—	—	—
	1975–1979	561	30.0	51.0	78.0	201.0	—	—
Wilson (1987)	1975	850	16.6	38.7	62.7	—	—	18.1
Barlas & Altaş[4] (1992)	1947–1990	3569	24.0	38.0		78.0 (≥2)		—
Present paper	1975–1999	75 739	18.9	35.7	66.3	116.0	—	20.6

[1] The smaller values attribute to less intense, the larger values to more intense flares.
[2] Duration calculated on the basis of photometric light curves.
[3] Only great solar flares were considered.
[4] Only spotless flares were considered.

Table 8. Median values of event asymmetries for the different importance classes with 95% confidence intervals. Furthermore, the absolute median deviations and the 10th percentiles are listed. For further discussions see the text.

Imp.	Event asymmetries		
	$\tilde{x} \pm c_{95}$	$\tilde{D}$	P_{10}
S	0.571 ± 0.003	0.238	0.00
1	0.615 ± 0.008	0.189	0.13
>1	0.682 ± 0.021	0.152	0.21
T	0.579 ± 0.003	0.226	0.00

Table 9. Comparison of the average monthly flare rate for solar cycles 21 and 22.

Imp.	cycle 21	cycle 22
S	388.6	259.2
1	34.6	37.2
>1	4.2	4.9
T	427.4	301.3

4.3. Dependency on the solar cycle

4.3.1. Number of flares

In Fig. 4 we plot the monthly number of Hα flares and the monthly mean Sunspot Numbers for the whole period of January 1975 to December 1999. The correlation coefficient of the Sunspot Numbers with the total number of flares occurring per month gives a value of ≈0.93, evidence that the occurrence of Hα flares is in strong coincidence with the solar cycle.

Figure 5 shows the monthly number of flares separately for the different importance classes. It is noteworthy that, although cycles 21 and 22 do not differ remarkably regarding the Sunspot Numbers, there is a significant difference in the flare occurrence rate (see Figs. 4 and 5). For the two solar cycles, which are totally covered by the data, i.e. solar cycle 21 (June 1976–August 1986) and solar cycle 22 (August 1986–April 1996), we list the average monthly rate of Hα flares per cycle (Table 9). On the one hand, solar cycle 21 reveals a conspicuously higher rate of subflares (which is also responsible for the higher rate of the total of flares). On the other hand, solar cycle 22 shows a higher rate of energetic flares, i.e. events of importance ≥1.

This fact that a cycle with a high rate of subflares produces a smaller number of major flares than a cycle with less subflares might be related to the mechanism of energy storage and release during solar flares. In order to

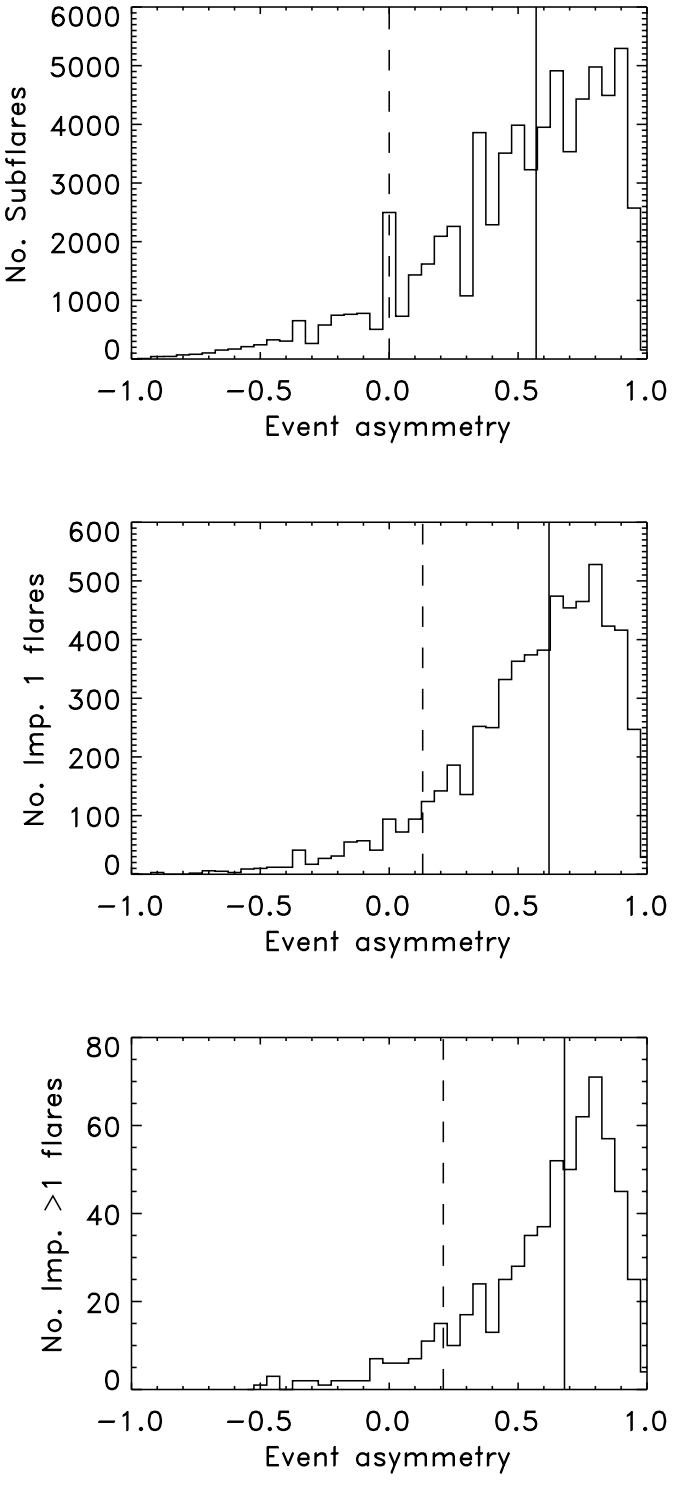

Fig. 3. Histograms of the event asymmetries, separately for importance classes S, 1 and >1. The solid line indicates the median of the distribution, the dashed line the 10th percentile P_{10}, which indicates that only 10% of the events have a value smaller than P_{10}.

produce a large flare, an active region must first store a vast amount of energy, which takes some time. The release of this energy during a flare occurs either due to an internal instability or an external destabilization, which can be caused, e.g., by nearby emerging new magnetic flux or by

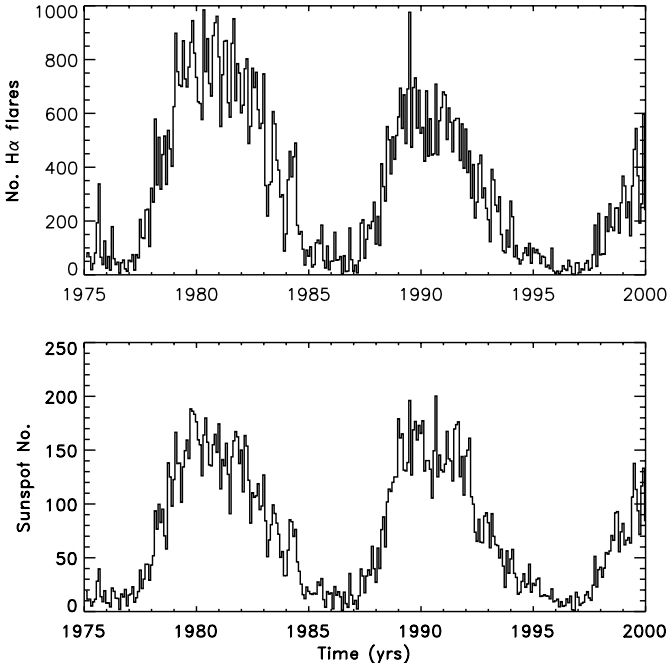

Fig. 4. Monthly number of Hα flares (top panel) and monthly mean Sunspot Numbers (bottom panel) for the period January 1975 to December 1999. The data of the monthly mean Sunspot Numbers are taken from the SGD.

a blast wave coming from another site of activity. Thus, if there are many small releases of magnetic energy in the form of subflares, there is little chance that enough energy can be stored before the energy storage site is destabilized (Švestka 1995).

4.3.2. Duration, rise and decay time

In Fig. 6 we plot the yearly median values of the flare duration, rise and decay times from 1975 to 1999. It can be clearly seen that each of the quantities reveals a trend to decreasing values. We have plotted a linear least squares fit superimposed on each of the time series in Fig. 6. Obviously, such a trend does not represent a physical phenomenon but we suggest that it is caused by observational selection effects. In particular, the time cadences of solar flare observations have increased with regard to former times, which enables us to detect more short-lived events. Further evidence for this explanation is provided by the comparison with a previous paper of the authors (Temmer et al. 2000), in which the temporal flare parameters of the subset 1994–1999 were investigated. For the flares of importance 1 and >1, the calculated duration values are very similar (the differences are of the order of the 95% confidence intervals) but for the subflares, to which most of the short-lived events belong, the average duration is distinctly shorter (≈10 min) than those obtained by the present analysis of the period 1975–1999 (≈14 min, see Table 5).

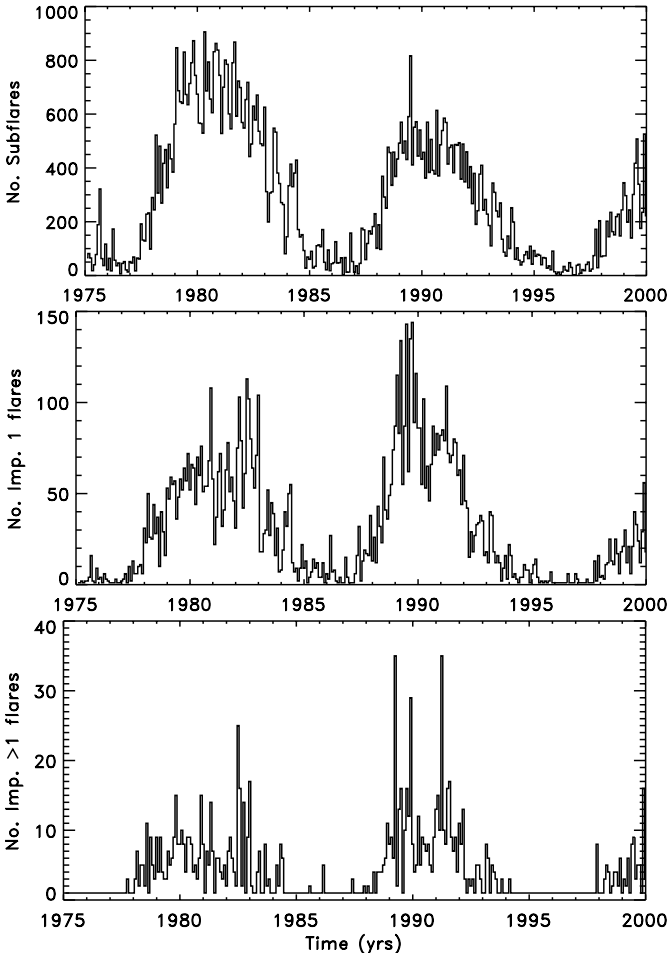

Fig. 5. Monthly number of Hα flares, separately for subflares (top panel), flares of importance 1 (middle panel) and importance >1 (bottom panel).

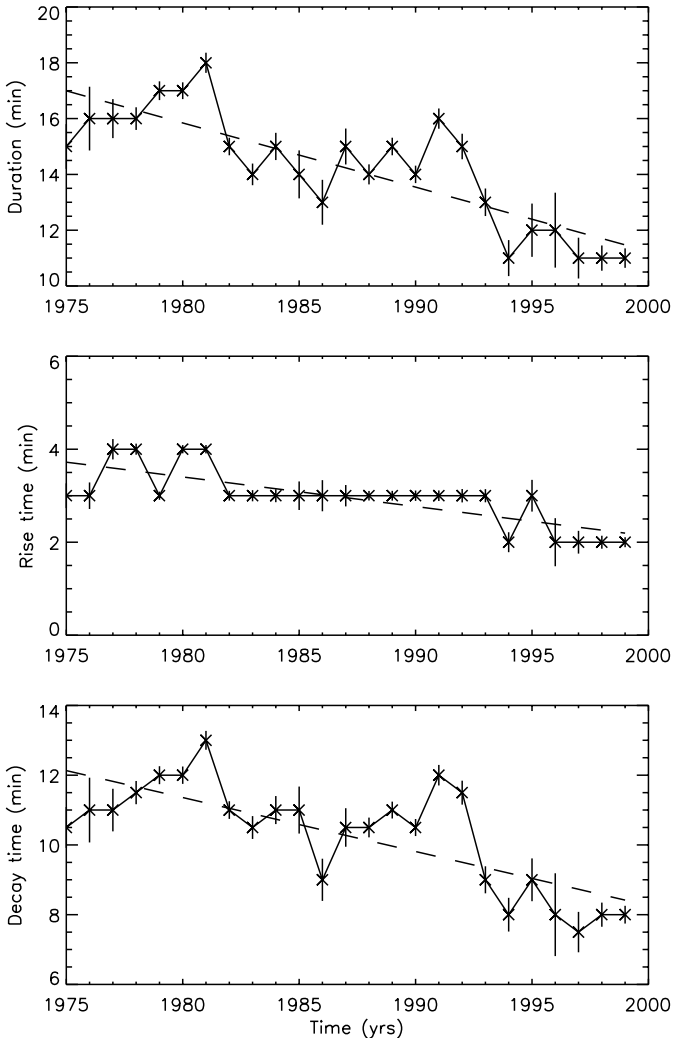

Fig. 6. Yearly median values of duration, rise and decay times. The error bars are given by the 95% confidence intervals, the dashed lines indicate a linear trend.

In order to find out if there is also a physical change in the duration, rise and decay times with the solar cycle, we subtracted the respective trends from the yearly duration, rise and decay time values and calculated the correlation coefficients with the yearly mean Sunspot Numbers (data taken from the SGD). The correlation coefficients yield quite high values for the duration as well as for the decay times, 0.71 and 0.73, respectively. For the rise times it is distinctly lower, with a value of 0.40. This means that the average duration and decay times are longer during times of maximum activity than during minimum phases, whereas the rise times do not show a noticeable variation with the solar cycle (see also the time series in Fig. 6). A similar behavior is pointed out by Wilson (1987), who performed a statistical study of flares occurring in the year 1980, i.e. around solar maximum (Wilson 1982a, 1982b, 1983), and in the year 1975, i.e. around solar minimum (Wilson 1987). He found a strong increase of the mean flare duration (1975: 18.1 ± 1.1 min, 1980: 29.8 ± 2.2 min) and decay time (1975: 12.9 ± 0.8 min, 1980: 22.1 ± 1.7 min), and a slighter but still pronounced increase of the mean rise time (1975: 5.2 ± 0.4 min, 1980: 7.7 ± 0.8 min) from solar minimum to maximum.

We want to stress that the outcome of the present analysis that the flare duration and decay times are significantly longer during times of solar maximum than during solar minimum is not caused by the fact that during maximum activity the number of large flares with long duration is higher, as the number of large flares is too low to significantly influence the overall statistics. However, to be sure, we repeated the analysis considering only subflares, which revealed the same behavior as the overall data set, i.e. a significant change of the duration and decay times in the course of the solar cycle.

4.3.3. Event asymmetry

In Fig. 7 we plot the yearly median values of the event asymmetries, defined by Eq. (1). The time series reveals a positive trend, resulting from the different trends of the rise and decay times. Again, we calculated the correlation

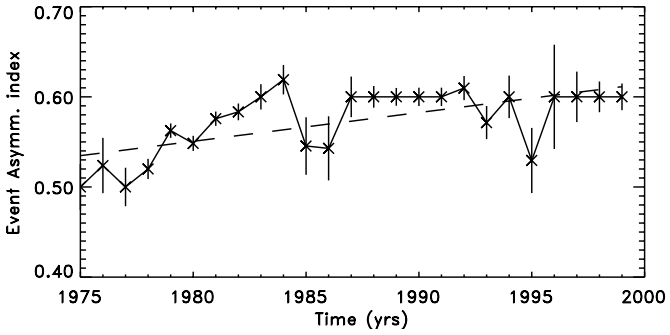

Fig. 7. Yearly median values of the event asymmetries. The error bars are given by the 95% confidence intervals, the dashed line indicates a linear trend.

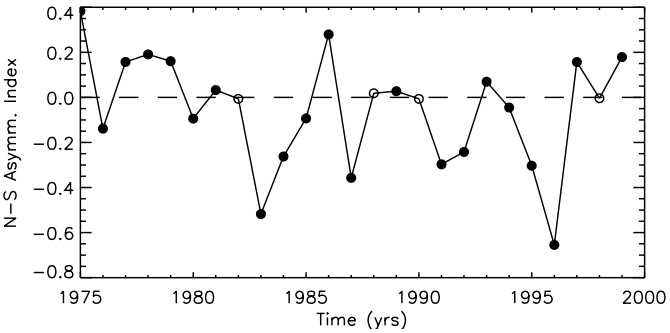

Fig. 8. Yearly N-S asymmetry index from 1975 to 1999. The significance of the N-S asymmetry values is specified by the plot symbols. Highly significant asymmetry values with $p \geq 99.5\%$ are marked with filled circles, otherwise white circles are drawn.

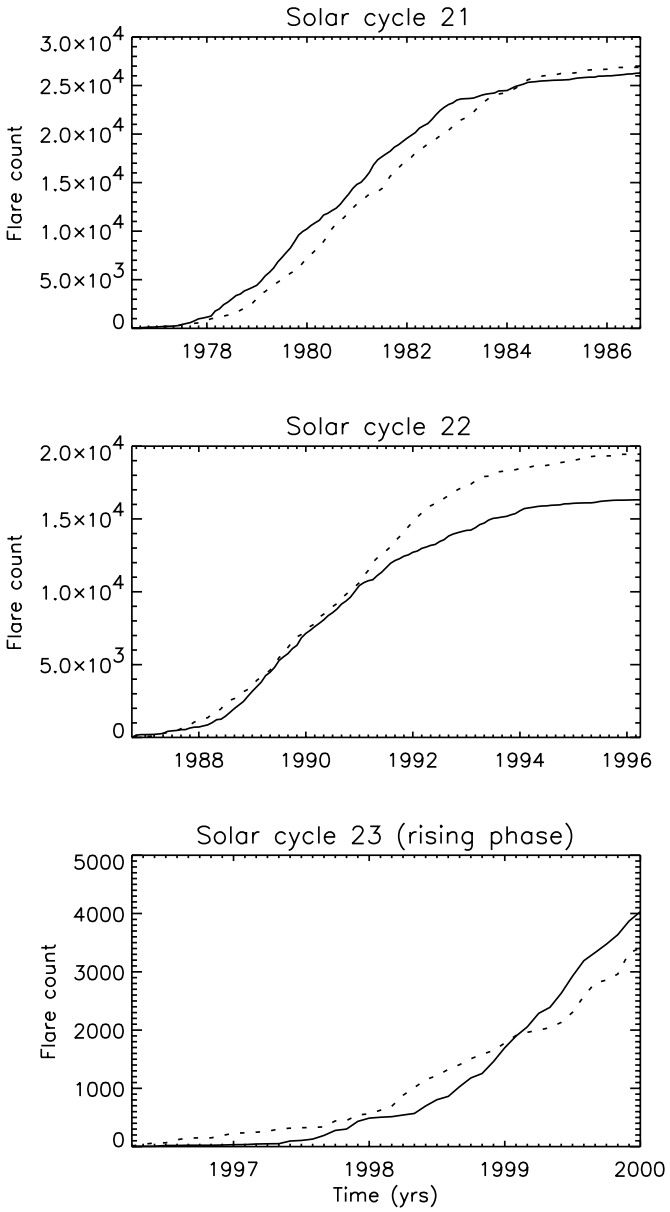

Fig. 9. Cumulative counts of flares occurring in the northern (solid lines) and the southern hemisphere (dashed lines) for solar cycles 21, 22 and 23. (For solar cycle 23 only the rising phase until the end of year 1999 is covered by the data.)

coefficient with the yearly mean Sunspot Numbers after subtraction of the trend, revealing no noticeable variation of the event asymmetries coincident with the solar cycle.

However, as can be seen in Fig. 7, during minima of solar activity the event asymmetries drop. This means that during times of low solar activity on average the energy build-up and decay of a flare takes place in a less asymmetric way than in other phases of the solar cycle. In order to check if this phenomenon is a statistical selection effect, induced by the low number of large flares during minimum activity, which have larger asymmetries than small ones (see Table 8), we repeated the analysis taking into account only subflares. The behavior remained qualitatively the same, suggesting that the decrease in the asymmetries during minimum activity is a real effect. The drop can be explained by the fact that the decay times are decreased during solar minimum phases but the rise times basically remain constant during the solar cycle.

4.3.4. North-South asymmetry

The existence of a N-S asymmetry of solar activity is generally accepted even if the phenomenon is still not satisfactorily interpreted. Several studies deal with the N-S asymmetry of various kinds of manifestations of solar activity, such as sunspots (Sunspot Numbers, areas, groups, magnetic classes, etc.), flares, prominences, radio bursts, hard X-ray bursts, gamma-ray bursts and coronal mass ejections. Investigations of the N-S asymmetry of solar flares have been carried out by Ružičková-Topolová (1974), Roy (1977), Knoška (1984), Verma (1987), Garcia (1990), Viktorinová & Antalová (1991), Joshi (1995), Ataç & Özgüç (1996), Li et al. (1998) and Ataç & Özgüç (2001). All papers reveal the existence of a N-S asymmetry; however, there are different outcomes if the evolution of the N-S asymmetry is correlated with the solar cycle or not.

In Fig. 8 we plot the yearly N-S asymmetry index, defined by Eq. (2), for the years 1975–1999. 21 out of 25 asymmetry values turn out to be highly significant,

with a probability $p \geq 99.5\%$ that the observed asymmetry index exceeds the dispersion value of a random distribution. The correlation coefficient calculated from the N-S asymmetry time series and the yearly mean Sunspot Numbers is very low, showing that the N-S asymmetry does not evolve in coincidence with the solar cycle.

In Fig. 9 we give another kind of representation of the N-S distribution, which was applied by Garcia (1990) to soft X-ray flares. In the figure, the cumulative number of flares occurring in the northern (solid lines) and the southern hemisphere (dashed lines) during solar cycles 21 and 22 and the rising phase of solar cycle 23 is plotted. The vertical spacing between the two lines is a measure of the northern/southern excess of Hα flares up to that time.

As Fig. 9 reveals, for solar cycle 21 an excess of flares occurring in the northern hemisphere develops during the rising phase of the cycle, staying roughly constant during the phase of major activity. About three years before the end of the cycle the northern excess degenerates and finally a very slight southern excess remains (50.6% south, 49.4% north). A same behavior but with a more pronounced spacing was found by Garcia (1990) for soft X-ray flares $\geq$ M9 (see his Fig. 1), who concluded from that result that the N-S asymmetry evolves in phase with the solar cycle. Viktorinová & Antalová (1991), who analyzed soft X-ray LDE (long duration event) flares during solar cycle 21 also found that the larger number of flares in the northern hemisphere is basically compensated by increased flare activity in the southern hemisphere in the declining phase of the cycle.

However, for solar cycle 22 the situation is quite different, as can be seen in Fig. 9. During the rising and maximum phase of the cycle a slight southern excess is present, which is strongly enhanced during the declining phase. Finally, for the whole cycle a distinct southern excess remains (54.4% south, 45.6% north). A southern flare dominance during solar cycle 22 was also obtained by Joshi (1995) for Hα flares and by Li et al. (1998) for soft X-ray flares $\geq$ M1. However, both studies were constrained to the maximum phase of the cycle.

Considering the whole time period from the beginning of year 1975 to the end of year 1999, a change in the predominance of flare occurrence in the northern and southern hemisphere can be detected. During most of solar cycle 21, the northern hemisphere was predominant. At the end of the cycle the dominance shifted to the southern hemisphere, which prevailed also during the whole of solar cycle 22. In the course of solar cycle 23 it seems that after a strong peak of the N-S asymmetry indicating a pronounced southern excess during the minimum phase 1996, the predominance again shifts to the northern hemisphere (see Figs. 8 and 9). The preference for the northern hemisphere during the rising phase of solar cycle 23 is also reported by Ataç & Özgüç (2001), who analyzed the N-S asymmetry of the solar flare index. However, as no unique relationship between the N-S asymmetry index as well as the cumulative northern/southern flare counts and the solar cycle can be found, the issue of whether the N-S asymmetry is in phase with the solar cycle remains ambiguous.

4.3.5. East-West asymmetry

The existence of an E-W asymmetry of solar activity is a more controversial issue than that of a N-S asymmetry. Since the E-W distribution depends on the reference position, there is no obvious physical reason why an E-W asymmetry should exist for longer periods (Heras et al. 1990). However, several authors (Letfus 1960; Letfus & Ružičková-Topolová 1980; Knoška 1984; Joshi 1995) found evidence for the existence of a small but significant E-W asymmetry in the occurrence of Hα flares. Heras et al. (1990) pointed out that the flare events are not uniformly spread in longitude, stressing that this fact has no influence on the E-W asymmetry but may be attributed to the transit of active zones on the solar disk. However, Heras et al. (1990) also found periods of pronounced and prolonged E-W asymmetry, which exceed the expectations from pure random fluctuations. Li et al. (1998), who studied the E-W asymmetry of soft X-ray flares, found slight E-W asymmetries, which they evaluated as not significant. However, they pointed out that the flares are not uniformly distributed over the visible longitude range.

In Fig. 10 we plot the yearly E-W asymmetry index, for the period 1975 to 1999. Even if the E-W asymmetry values are rather low, 18 out of 25 asymmetry values reveal a high statistical significance with $p \geq 99.5\%$. A comparison with Fig. 8 shows that the E-W asymmetry is obviously lower than the N-S asymmetry. However, the E-W asymmetry also can be quite pronounced during certain periods, e.g., during the minimum phase in 1996 the E-W asymmetry reveals a strong negative peak, indicating a distinct western excess. At the same time, the N-S asymmetry reveals a strong southern excess. An enhancement of the N-S and E-W asymmetry during solar minima has already been reported in several papers (Roy 1977; Knoška 1984; Heras et al. 1990; Joshi 1995; Ataç & Özgüç 1996). However, we can validate this effect only for the solar minimum in 1996. Moreover, as the correlation coefficient of the N-S asymmetry time series and the yearly mean Sunspot Numbers is very low, there is no indication that in general the E-W asymmetry evolves in phase with the solar cycle.

In Fig. 11 the cumulative number of flares occurring in the eastern (solid lines) and the western hemisphere (dashed lines) during solar cycles 21 and 22 and the rising phase of solar cycle 23 is plotted. Solar cycle 21 and 22 reveal a rather similar behavior. Except for the early phases of the cycles, a slight but continuously increasing eastern excess develops. The final excess amounts to 51.2% east, 48.8% west for solar cycle 21 and 51.5% east, 48.5% west for cycle 22. For solar cycle 23, only a part of the ascending phase is covered by the data. During this phase, a western excess developed. However, this western excess may

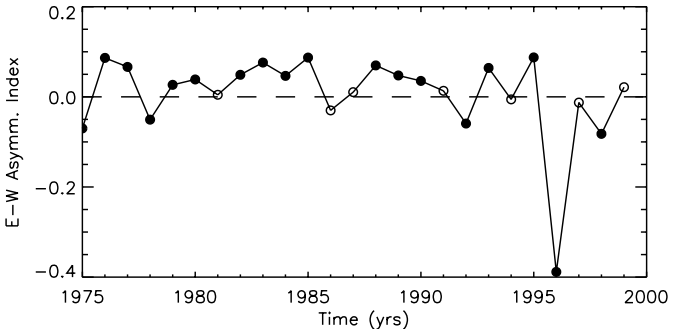

Fig. 10. Yearly E-W asymmetry index from 1975 to 1999. Highly significant asymmetry values with $p \geq 99.5\%$ are indicated by filled circles.

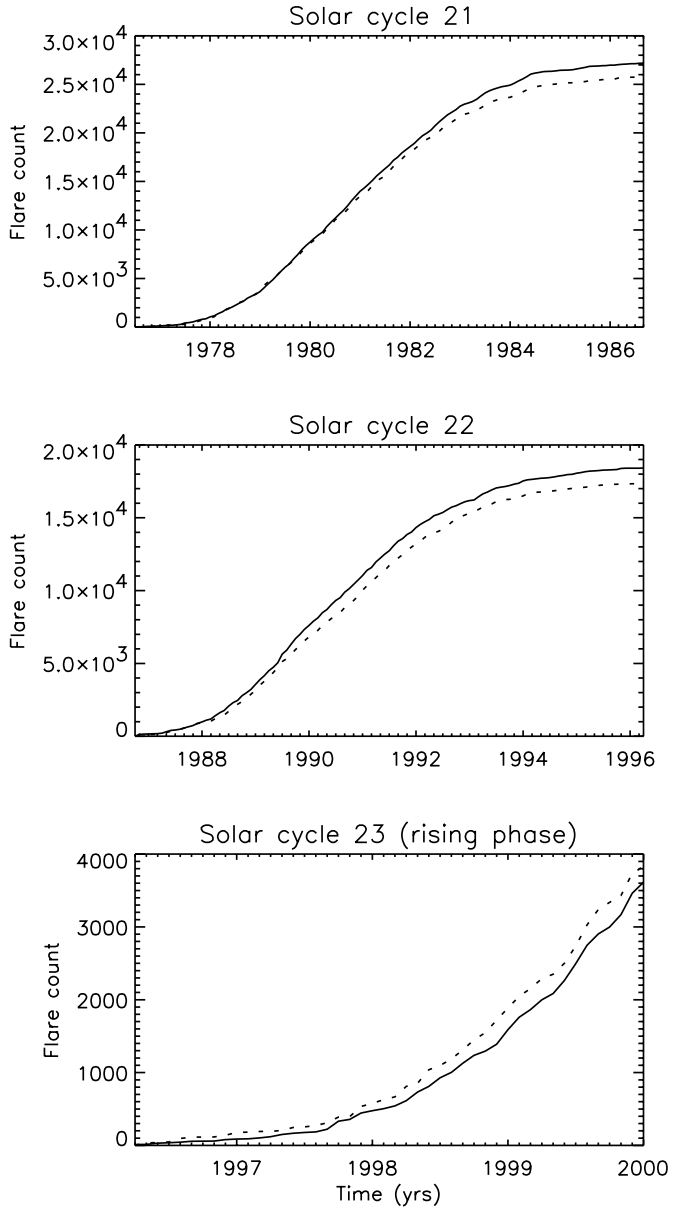

Fig. 11. Cumulative counts of flares occurring in the eastern (full lines) and the western hemisphere (dashed lines) for solar cycles 21, 22 and 23 (until the end of year 1999).

be overruled by the following years of maximum activity, since the number of flares at the end of 1999 covers just about 15–20% of the overall flare number, which can be expected for the whole cycle. Therefore, no definitive conclusion about the E-W asymmetry of solar cycle 23 can be drawn.

Comprising previous investigations of the E-W asymmetry of solar flares and the present paper, solar cycles 17 to 22 are covered by the analysis (Letfus 1960: 1935–1958; Ružičková-Topolová 1974: 1957–1965; Letfus & Ružičková-Topolová 1980: 1959–1976; Knoška 1984: 1937–1978; Heras et al: 1990: 1976–1985; Joshi 1995: 1989–1991; Li et al. 1998: 1987–1992; present paper: 1975–1999). Considering only those papers in which the found E-W asymmetries are evaluated as significant, it is worthwhile to mention that for longer periods, almost all authors find an excess of flares in the eastern hemisphere. Thus, possibly a low but prolonged dominance of the eastern hemisphere existed during solar cycles 17 to 22, which is a rather surprising outcome.

5. Summary and conclusions

5.1. Temporal parameters

The main results of the analysis regarding temporal flare parameters, as duration, rise times, decay times and event asymmetries are summarized in the following. 1) On average, the duration, rise and decay times of flares increase with increasing importance class. The increase is more pronounced for the decay times (factor 4–5 between subflares and flares of importance >1) than for the rise times (factor 2–3). The same relation holds for the brightness classes but in a weaker manner. 2) The event asymmetries, which characterize the proportion of the decay to the rise time of a flare, are predominantly positive (≈90%). For more than 50% of all flares the decay phase is even more than 4 times as long as the rising phase. 3) On average, the event asymmetries increase with the importance class. 4) The duration changes in phase with the solar cycle, i.e. on average the flare duration is longer during periods of maximum activity than during solar minima. Since the rise times do not reveal a distinct correlation with the solar cycle but the decay times do, the variations of the duration in accordance with the solar cycle are due to the variations of the decay times. 5) The event asymmetries do not reveal a distinct correlation with the solar cycle. However, they decrease during solar minima.

The facts that on the average the flare duration increases with the importance class and the rise times are shorter than the decay times are reported in a number of previous papers (see the references cited in Table 7). However, the new outcome of the present analysis is, on the one hand, that the increase of the duration with the importance class in particular results from the increase of the decay times, which is significantly more pronounced than the increase of the rise times. On the other hand, by the concept of the event asymmetry, we were able to give

a quantitative description of the asymmetry in the flare development, which revealed that on average the asymmetry also increases with the importance class. Both results suggest that, with respect to the temporal behavior, the cooling phase of the Hα flare is more strongly affected by the flare size than the phase of heating-up the chromospheric plasma at the flare site.

Furthermore, a significant change in the duration and decay times with the solar cycle was found. On average, during solar maximum the decay times are larger than during solar minimum, with $t_{\rm decay}^{\rm max} \approx 1.5 \cdot t_{\rm decay}^{\rm min}$. The rise times do not reveal a significant variation in accordance with the cycle. The combination of both facts can also account for the drop in the event asymmetries found during solar minima. These results suggest that the change in the flare duration is mainly caused by the variations of the decay times, giving further evidence that the flare cooling phase is more sensitive to changes in the physical conditions of the chromospheric plasma than the rising phase.

5.2. Spatial distributions

The main outcomes of the present analysis regarding the spatial distribution of flares over the different hemispheres are: 1) There exists a significant N-S asymmetry over longer periods, and the dominance of one hemisphere over the other can persist for more than one cycle. 2) For certain cycles there may be evidence that the N-S asymmetry evolves in coincidence with the solar cycle, but in general this is not the case. 3) There exists a slight but significant E-W asymmetry with a prolonged eastern excess during solar cycles 21 and 22. Combining the results obtained by previous authors and the present paper, possibly an eastern excess of solar flares existed during solar cycles 17 to 22.

The existence of a N-S asymmetry is generally accepted but still not definitely interpreted. One possible explanation of the N-S asymmetry of solar activity phenomena is that a time difference in the development of solar activity on the northern and the southern hemisphere exists (e.g., Tritakis et al. 1997). However, in this case the N-S asymmetry is expected to evolve in coincidence with the solar cycle, which is rather ambiguous. Another explanation utilizes the concept of "superactive regions", which are large, complex, active regions containing sunspots (Bai 1987, 1988). Such superactive regions produce the majority of solar flare events and appear preferentially in certain areas of the Sun, so-called "active zones". As shown by Bai et al. (1988), in the past active zones were present on the Sun, which persisted for several solar cycles. In that frame, the N-S asymmetry can be attributed to the existence of active zones in the northern and southern hemispheres, which can persist over long periods.

Also the fact that flares are not uniformly spread in heliographic longitude over the solar disk (note that this non-uniformity has a different meaning than the E-W asymmetry), pointed out by Heras et al. (1990) and Li et al. (1998), can be understood in the framework of the active zones concept. The longitudes, at which the active zones are located, are more flare-productive than other longitude ranges. The active zones induce a pronounced and non-random flare activity, which is superimposed onto an episodic and random flare activity coming from the other (less active) regions of the solar disk (Heras et al. 1990). However, the idea of active zones cannot account for an E-W asymmetry persisting over time scales larger than those of the solar rotation.

The first report of an E-W asymmetry in solar activity was given by Maunder (1907), who found that the total spot area and total number of spot groups were larger in the eastern than in the western hemisphere. A possible interpretation of this effect was given by Minnaert (1946). A forward tilt of the vertical sunspot axis causes a "physical" foreshortening of the spots, which acts more strongly on spots on the western than on those on the eastern hemisphere. However, it cannot be seen how such an effect could also account for an eastern excess in the flare occurrence rate. In recent papers (Mavromichalaki et al. 1994; Tritakis et al. 1997) it has also been found that the emission of the eastern hemisphere of the corona systematically predominates. However, the coronal E-W asymmetry as well as the E-W asymmetry of solar flares are still unexplained and controversial issues.

Acknowledgements. The authors thank Helen Coffey and Craig Clark from NGDC for making available the Hα flare data of the SGD. M. T., A. V. and A. H. gratefully acknowledge the Austrian *Fonds zur Förderung der wissenschaftlichen Forschung* (FWF grant P13655-PHY) for supporting this project. M.M. acknowledges the support by ASI and MURST.

References

Antalová, A. 1985, Contr. Astr. Obs. Skalnaté Pleso, 13, 243
Ataç, T., & Özgüç, A. 1996, Solar Phys., 166, 201
Ataç, T., & Özgüç, A. 2001, Solar Phys., 198, 399
Bai, T. 1987, ApJ, 314, 795
Bai, T. 1988, ApJ, 328, 860
Barlas, O., & Altas, L. 1992, Astrophys. Space Sci., 197, 337
Cliver, E. W. 1995, Solar Phys., 157, 285
Dodson, H. W., Hedeman, E. R., & McMath, R. R. 1956, ApJS, 20, 241
Ellison, M. A. 1949, MNRAS, 109, 3
Garcia, H. A. 1990, Solar Phys., 127, 185
Giovanelli, R. G. 1948, MNRAS, 108, 163
Heras, A. M, Sanahuja, B., Shea, M. A., & Smart, D. F. 1990, Solar Phys., 126, 371
Joshi, A. 1995, Solar Phys., 157, 315
Knoška, Š. 1984, Contr. Astr. Obs. Skalnaté Pleso, 13, 217
Letfus, V. 1960, Bull. Astron. Inst. Czechosl., 11, 31
Letfus, V., & Ružičková-Topolová, B. 1980, Bull. Astron. Inst. Czechosl., 31, 232
Li, K.-J., Schmieder, B., & Li, Q.-Sh. 1998, A&AS, 131, 99
Maunder, A. S. D. 1907, MNRAS, 67, 451
Mavromichalaki, H., Tritakis, V., Petropoulos, B., et al. 1994, Astrophys. Space Sci., 218, 35
Minnaert, M. G. J. 1946, MNRAS, 106, 98

Newton, H. W., & Barton, H. J. 1937, MNRAS, 97, 594
Pearce, G., Lee, R., Herrington, S., & Parker, J. 2001, A Analysis of Solar Data in the Soft X-Ray and Optical Wavelengths, in Recent Insights into the Physics of the Sun and Heliosphere: Highlights from SOHO and Other Space Missions, Proc. IAU Symp. 203, ed. P. Brekke, B. Fleck, & J. B. Gurman, in press
Reid, J. H. 1968, Solar Phys., 5, 207
Roy, J.-R. 1977, Solar Phys., 52, 53
Ružičková-Topolová, B. 1974, Bull. Astron. Inst. Czechosl., 25, 345
Smith, H. J. 1962, G.R.D. Research Note A.F.C.R.L., 62, 827
Švestka, Z. 1995, Adv. Space Res., 16(9), 27
Temmer, M., Veronig, A., Hanslmeier, A., et al. 2000, Hvar Obs. Bull., 24, 185
Tritakis, V., Mavromichalaki, H., Paliatsos, A. G., Petropoulos, B., & Noens, J. C. 1997, New Astr., 2, 437
Verma, V. K. 1987, Solar Phys., 114, 185
Viktorinová, B., & Antalová, A. 1991, Bull. Astron. Inst. Czechosl., 42, 144
Waldmeier, M. 1938, Z. Astrophys., 16, 276
Waldmeier, M. 1948, Astron. Mitt. Zürich, 153
Waldmeier, M., & Bachmann, H. 1959, Z. Astrophys., 47, 81
Warwick, C. S. 1954, ApJ, 120, 237
Wilson, R. M. 1982a, NASA Techn. Memo. 82465, Marshall Space Flight Center, Alabama
Wilson, R. M. 1982b, NASA Techn. Memo. 82475, Marshall Space Flight Center, Alabama
Wilson, R. M. 1983, NASA Techn. Memo. 82526, Marshall Space Flight Center, Alabama
Wilson, R. M. 1987, NASA Techn. Paper, TP-2714
Yeung, J., & Pearce, G. 1990, A&AS, 82, 543